

# Towards Precise Intra-camera Supervised Person Re-identification

Menglin Wang<sup>1</sup>, Baisheng Lai<sup>2</sup>, Haokun Chen<sup>1</sup>,  
Jianqiang Huang<sup>2</sup>, Xiaojin Gong<sup>1</sup>, Xian-Sheng Hua<sup>2</sup>

<sup>1</sup>Zhejiang University, Hangzhou, China

<sup>2</sup>Alibaba Group, Hangzhou, China

lynnwang6875@gmail.com, baisheng.lbs@alibaba-inc.com, chenhaokun@zju.edu.cn,  
jianqiang.hjq@alibaba-inc.com, gongxj@zju.edu.cn, huaxiansheng@gmail.com

## Abstract

Intra-camera supervision (ICS) for person re-identification (Re-ID) assumes that identity labels are independently annotated within each camera view and no inter-camera identity association is labeled. It is a new setting proposed recently to reduce the burden of annotation while expect to maintain desirable Re-ID performance. However, the lack of inter-camera labels makes the ICS Re-ID problem much more challenging than the fully supervised counterpart. By investigating the characteristics of ICS, this paper proposes camera-specific non-parametric classifiers, together with a hybrid mining quintuplet loss, to perform intra-camera learning. Then, an inter-camera learning module consisting of a graph-based ID association step and a Re-ID model updating step is conducted. Extensive experiments on three large-scale Re-ID datasets show that our approach outperforms all existing ICS works by a great margin. Our approach performs even comparable to state-of-the-art fully supervised methods in two of the datasets.

## 1 Introduction

Person re-identification (Re-ID) is the task of matching images of the same person across disjoint cameras. Because of its significance in surveillance, this task has attracted broad research interest in recent years. Most previous works focus on fully supervised [Sun *et al.*, 2018; Zhang *et al.*, 2019; Chen *et al.*, 2019; Luo *et al.*, 2019] and unsupervised [Deng *et al.*, 2018; Zhong *et al.*, 2019a; Fan *et al.*, 2018; Wu *et al.*, 2019] settings. The performance of supervised person Re-ID has been greatly improved due to the development of deep learning techniques. However, these methods need a large amount of full annotations that are expensive and time-consuming to obtain, making them unscalable to real-world applications. Conversely, unsupervised methods require no annotations but their performance is still far from satisfactory.

This paper aims to learn a person Re-ID model under intra-camera supervision (ICS), which is a supervised setting proposed very recently [Zhu *et al.*, 2019; Qi *et al.*, 2019b]. It assumes that identity labels are independently annotated within

each camera and no inter-camera identity association is labeled. Since the ID association across cameras is known as the most time-consuming part for manual annotation, ICS can greatly save annotation costs and make the Re-ID techniques more scalable. Nevertheless, the lack of inter-camera labels brings up more challenges when dealing with appearance variations in different cameras, leading to a performance inferior to the supervised counterparts.

In order to bridge the performance gap, we address the ICS person Re-ID problem by adopting the BNNeck [Luo *et al.*, 2019] augmented ResNet-50 [He *et al.*, 2016], which is simple but shown to be effective in the fully supervised Re-ID task, as our backbone. Upon the backbone we construct two branches, respectively, for intra- and inter-camera learning. The intra-camera learning aims to learn a discriminative feature representation via leveraging the per-camera annotations. In ICS, the per-camera independent labeling manner results in some identity classes containing only a few instances. Concerning this characteristic, we exploit non-parametric classifiers [Xiao *et al.*, 2017; Wu *et al.*, 2018] and design a camera-specific way to perform ID classification within each camera view. The non-parametric classifiers are implemented via an external memory bank, which additionally inspires us to propose a quintuplet loss. This loss takes advantage of information within each mini-batch and over global training batch to boost the intra-camera learning performance. The inter-camera learning aims to improve the Re-ID model by mining ID relationships across cameras. To this end, we design a graph-based strategy for ID association and pseudo labeling, which are further used to learn a better Re-ID model by directly training the BNNeck augmented network in a fully supervised manner.

Although both intra- and inter-camera learning perspectives are considered in existing ICS works [Qi *et al.*, 2019a; Qi *et al.*, 2019b; Zhu *et al.*, 2019], our approach distinguishes itself from the others in the following aspects:

- We propose camera-specific non-parametric classifiers and a quintuplet loss for intra-camera learning. These designs are customized not only for the characteristics of ICS but also for the memory assisted network architecture. They enable our intra-camera learning module to achieve a Re-ID performance better than all existing ICS models that consider both intra- and inter-camera

learning parts.

- In inter-camera learning, our graph-based association step produces desirable pseudo labeling results, which enables us to directly apply the BNNeck augmented network architecture to train the Re-ID model in a fully supervised manner. Riding the wave of architectures successfully applied in the supervised Re-ID task boosts the performance further.
- Extensive experiments on three large-scale Re-ID datasets including Market-1501 [Zheng *et al.*, 2015], DukeMTMCreID [Ristani *et al.*, 2016; Zheng *et al.*, 2017], and MSMT17 [Wei *et al.*, 2018], show that the proposed approach outperforms previous ICS works by a great margin. Our performance is even comparable to fully supervised methods on the first two datasets.

## 2 Related Work

### 2.1 Person Re-identification

**Fully supervised person Re-ID** has made significant progress relying on the success of deep learning techniques. However, it remains to be an unsolved problem due to challenges arising from cluttered background, occlusion, as well as variations in illumination, pose, and viewpoint. Recent methods have exploited part-based features [Sun *et al.*, 2018], human semantics [Zhang *et al.*, 2019], attention mechanisms [Chen *et al.*, 2019], or data generation [Zheng *et al.*, 2019] to tackle the challenges. These methods often lead to complex network architectures. An exceptional work is Bag of Tricks (BoT) [Luo *et al.*, 2019] that achieves the state-of-the-art Re-ID performance by applying some training tricks on a baseline network. Inspired by it, we construct our network upon the BoT model, i.e. the BNNeck augmented ResNet-50, to keep our backbone simple yet effective.

**Unsupervised person Re-ID** has attracted a lot of research interest in recent years. Existing methods can be roughly categorized into two groups. One is based on domain adaptation techniques [Deng *et al.*, 2018; Zhong *et al.*, 2019a; Ding *et al.*, 2019] that transfer knowledge from labeled source domain to unlabeled target domain. The other group is purely unsupervised that requires no external labeled data. These methods usually perform a step to associate IDs across cameras via clustering [Fan *et al.*, 2018; Lin *et al.*, 2019] or graph [Wu *et al.*, 2019] based strategies. Our intra-camera supervised work also adopts a graph-based ID association step. But, in contrast to use a graph-weighted loss [Wu *et al.*, 2019], we formulate the association as a problem of finding connected components in a graph.

**Semi-supervised person Re-ID** aims to learn a Re-ID model from both labeled and unlabeled data [Yang *et al.*, 2019]. Intra-camera supervision (ICS) is a special semi-supervised setting proposed very recently. All existing ICS works address the Re-ID problem by considering both intra- and inter-camera learning parts. For supervised intra-camera learning, [Qi *et al.*, 2019a; Qi *et al.*, 2019b] take the extensively used triplet loss [Hermans *et al.*, 2017] while [Zhu *et al.*, 2019] designs a

multi-branch structure to learn classifiers. For inter-camera learning, [Qi *et al.*, 2019a] develops a multi-camera adversarial learning approach to reduce the cross-camera data distribution discrepancy, [Qi *et al.*, 2019b] utilizes a soft-labeling scheme, and [Zhu *et al.*, 2019] adopts a multi-label learning strategy. In contrast, we propose different learning strategies in both parts and achieve much higher Re-ID performance.

### 2.2 Parametric and Non-parametric Classifiers

**Parametric classifiers** in this work refer to those implemented by fully connected (FC) layers in a deep neural network (DNN), usually trained with a cross-entropy softmax classification loss. Such classifiers have been extensively used in fully supervised person Re-ID [Sun *et al.*, 2018; Zhai *et al.*, 2019; Luo *et al.*, 2019]. However, they have the following drawbacks: 1) The training process pays much attention on learning parameters for the FC layers that are abandoned during inference for person Re-ID [Zhai *et al.*, 2019], making the learned feature representation less discriminative for test data. 2) The classifiers can not be learned effectively when there are a large number of identities while each identity only has a small number of instances [Xiao *et al.*, 2017].

**Non-parametric classifiers** in a DNN are implemented via an external memory bank and a non-parametric variant of the softmax function. It is first proposed in a fully supervised person search task [Xiao *et al.*, 2017] and extensively adopted in unsupervised [Wu *et al.*, 2018; Zhong *et al.*, 2019a; Zhong *et al.*, 2019b] and semi-supervised [Chen *et al.*, 2018; Yang *et al.*, 2019] learning. A common challenge in these tasks is that the number of classes is huge but each class contains only one or few examples. A DNN equipped with the non-parametric classifiers makes its parameters independent to the class number so that the training process entirely focus on the feature representation learning. Nevertheless, the non-parametric model may overfit more easily when training data is abundant enough.

## 3 The Proposed Method

The intra-camera supervision assumes that identity labels are independently annotated within each camera view and no inter-camera identity association is provided. Suppose there are  $C$  cameras in a dataset. We denote the set of the  $c$ -th camera by  $\mathcal{D}_c = \{(x_i, y_i, c_i)\}_{i=1}^{M_c}$ , in which image  $x_i$  is annotated with an identity label  $y_i \in \{1, \dots, N_c\}$  and a camera label  $c_i = c \in \{1, \dots, C\}$ .  $M_c$  and  $N_c$  are, respectively, the number of total images and IDs in this camera view.  $N = \sum_{c=1}^C N_c$  is the total ID number directly accumulated over all cameras. It should be noted that the identities in different cameras are partially overlapped. That is, a same person may appear in two or more camera views, but it could be assigned with different IDs due to the per-camera independent labeling manner. Given this training set  $\mathcal{D} = \bigcup_{c=1}^C \mathcal{D}_c$ , we aim to learn a person Re-ID model that can well discriminate both intra- and inter-camera identities.

To this end, we develop our method from both intra- and inter-camera learning perspectives. The overall framework is shown in Figure 1. An image is first fed into a backbone

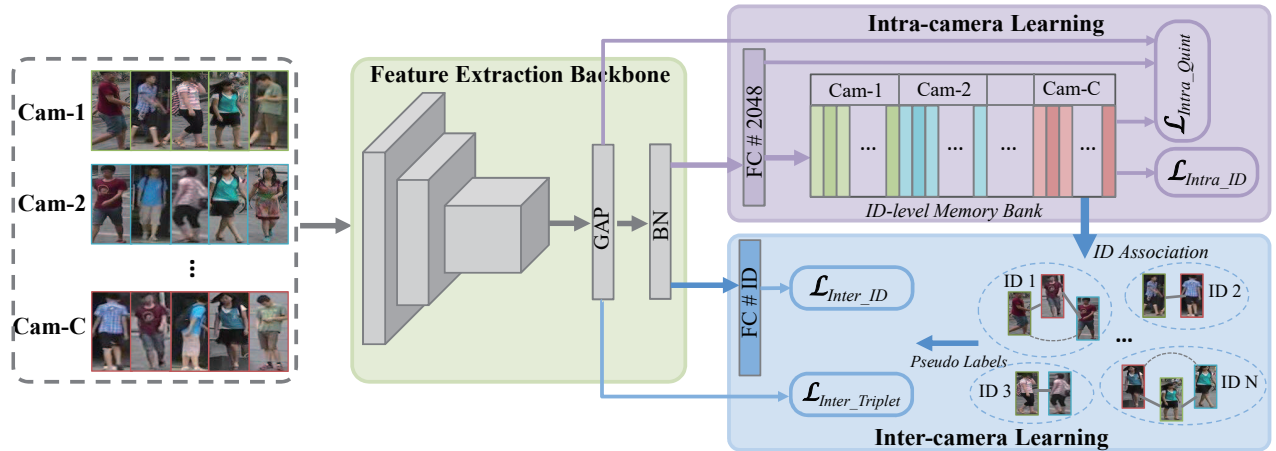


Figure 1: An overview framework of the proposed method. It consists of a feature extraction backbone, together with an intra-camera learning branch and an inter-camera learning branch. In intra-camera learning, features are classified via camera-specific non-parametric classifiers implemented via an external memory bank, optimized by  $\mathcal{L}_{Intra\_ID}$  and  $\mathcal{L}_{Intra\_Quint}$ . In inter-camera learning, IDs are associated across cameras and pseudo labeled, which are further used to update the Re-ID model by optimizing  $\mathcal{L}_{Inter\_ID}$  and  $\mathcal{L}_{Inter\_Triplet}$ .

network for feature extraction. The extracted feature goes through an additional feature embedding layer and then classified by camera-specific non-parametric classifiers that are implemented via an external memory bank, together with an ID classification loss and a quintuplet loss, for intra-camera learning. The memory bank stores the centroid feature of each ID, which is of moderate discrimination ability after intra-camera learning. Then, the ID centroids are used for ID association and pseudo labeling across cameras. In inter-camera learning, the same backbone is adopted to extract features, along with a classifier parameterized by a FC layer to classify images into their pseudo identity classes.

### 3.1 Intra-camera Learning

When considering the Re-ID problem within an individual camera view, it can be treated as a fully supervised classification task. Therefore, it is reasonable to formulate the intra-camera learning as a multi-task classification problem and adopt a multi-branch architecture as done in [Zhu *et al.*, 2019]. The network architecture is designed to share a feature extraction backbone and append with multiple classification branches, each of which corresponds to a specific camera view. This architecture is capable of learning feature representations that are discriminative within cameras and also somewhat discriminative across cameras. However, the parametric classifiers implemented via fully-connected layers in the branches could become ineffective when some IDs contain only a couple of samples, which is a common situation in the intra-camera supervised setting.

#### Camera-specific Non-parametric Classifiers

To alleviate the above-mentioned problem, we adopt non-parametric classifiers for intra-camera learning. As illustrated in Figure 1, our network consists of a feature extraction backbone, a FC embedding layer, together with an external memory bank. Based upon this network structure, we design camera-specific non-parametric classifiers to perform

the classification tasks within each camera view.

Formally, when an image is input, the FC embedding layer outputs a  $d$ -dimensional feature vector. The memory bank  $\mathcal{K} \in R^{d \times N}$  stores the up-to-date features of all accumulated IDs and each column corresponds to one ID. During back-propagation, the memory bank is updated by

$$\mathcal{K}[j] \leftarrow \mu \mathcal{K}[j] + (1 - \mu) f(x_i), \quad (1)$$

where  $\mathcal{K}[j]$  is the  $j$ -th column of the memory.  $f(x_i)$  is a  $L_2$  normalized feature extracted from image  $x_i$  that belongs to the  $j$ -th ID.  $\mu \in [0, 1]$  is an updating rate. After each update,  $\mathcal{K}[j]$  is scaled to having unit  $L_2$  norm. The updated feature in each column can be interpreted as the centroid of an identity class in the feature space, which is a  $d$ -dimensional unit hypersphere.

Given the image  $x_i$ , together with its annotated intra-camera identity label  $y_i$  and camera label  $c_i$ . The corresponding global ID index  $j$  is obtained by  $j = A + y_i$ , where  $A = \sum_{k=1}^{c_i-1} N_k$  is the total ID number accumulated from the first to the  $c_i - 1$ -th camera view. Then, the probability of classifying  $x_i$  into the  $j$ -th ID is defined by a non-parametric softmax function

$$p(j|x_i) = \frac{\exp(\mathcal{K}[j]^T f(x_i)/\tau)}{\sum_{k=A+1}^{A+N_{c_i}} \exp(\mathcal{K}[k]^T f(x_i)/\tau)}, \quad (2)$$

where  $\tau$  is the temperature controlling the smoothness of probability distribution.

Note that the non-parametric classifier defined above is camera-specific, because the sum in the denominator is over the IDs within the same camera view only. In contrast to existing works [Xiao *et al.*, 2017; Wu *et al.*, 2018; Zhong *et al.*, 2019a; Ding *et al.*, 2019] that considers all entries in their memory bank, our formulation only takes those belonging to the same camera into account while ignores the IDs in all other cameras. Thus, each non-parametric classifier is responsible for the classification task within a specific camera.

The objective of camera-specific ID classification, termed as the intra-camera ID loss, is to minimize the negative log-likelihood over all training images. That is,

$$\mathcal{L}_{Intra\_ID} = - \sum_{c=1}^C \left( \frac{1}{|\mathcal{D}_c|} \sum_{x_i \in \mathcal{D}_c} \log p(j|x_i) \right), \quad (3)$$

where the normalization coefficient  $\frac{1}{|\mathcal{D}_c|}$  is placed to balance the various number of images under different cameras.

### A Hybrid Mining Quintuplet Loss

Inspired by recent fully supervised methods [Luo *et al.*, 2019; Chen *et al.*, 2019; Zhang *et al.*, 2019] that combine ID loss and triplet loss together to learn precise Re-ID models, we also incorporate a metric learning loss as a supplement to the intra-camera ID loss to boost the performance. Instead of directly using the triplet loss that only samples locally within each mini-batch, we propose a quintuplet loss, which can take advantage of information not only in each mini-batch but also over the global training batch to enhance the intra-ID compactness and inter-ID separability.

Specifically, in each mini-batch, we randomly select  $P$  identities and  $K$  instances of each identity, as the common practice [Hermans *et al.*, 2017]. For each anchor image  $x_a$ , we design a hybrid mining scheme that selects two instances and two identity centroids to form a quintuplet. The positive and negative instances are sampled to be the hardest ones within a mini-batch. In addition, we choose the positive ID centroid and the nearest negative ID centroid from the memory bank. Note that all instances and centroids are selected from the same camera as the anchor. Then, the intra-camera quintuplet loss is defined as follows:

$$\begin{aligned} \mathcal{L}_{Intra\_Quint} = & \sum_{i=1}^P \sum_{a=1}^K \left[ m_1 + \max_{p=1, \dots, K} \|g(x_a^i) - g(x_p^i)\| \right. \\ & - \min_{n=1, \dots, K; j=1, \dots, P; j \neq i; c_a^i = c_n^j} \|g(x_a^i) - g(x_n^j)\| \Big]_+ \\ & + \left[ m_2 + \|f(x_a^i) - \mathcal{K}[A + y_a^i]\| \right. \\ & - \min_{j=1, \dots, N; c_a^i: j \neq y_a^i} \|f(x_a^i) - \mathcal{K}[A + j]\| \Big]_+, \quad (4) \end{aligned}$$

where  $m_1$  and  $m_2$  are two margins.  $g(x_a)$ ,  $g(x_p)$ , and  $g(x_n)$  are, respectively, the features of the anchor, positive and negative instances output from the global average pooling (GAP) layer in the backbone.  $f(x_a)$  is the anchor's feature produced from the FC embedding layer as above-mentioned. Taking features from different layers is inspired by the BNNeck structure in [Luo *et al.*, 2019] and shown to be effective in our experiments. In addition,  $A + y_a$  is the global ID index in  $\mathcal{K}$  given the intra-camera ID  $y_a$ ,  $[\cdot]_+ = \max(0, \cdot)$ , and  $\|\cdot\|$  is the Euclidean distance.

### The Loss for Intra-camera Learning

In summary, the loss for intra-camera learning is the sum of the camera-specific ID classification loss and the quintuplet loss:

$$\mathcal{L}_{Intra} = \mathcal{L}_{Intra\_ID} + \mathcal{L}_{Intra\_Quint}. \quad (5)$$

## 3.2 Inter-camera Learning

The Re-ID model trained via intra-camera learning achieves considerable discrimination capability. However, the lack of explicit inter-camera correlations renders the model relatively weak at coping with variations in different cameras. To address this problem, we perform an inter-camera learning that consists of a cross-camera ID association step and a Re-ID model updating step.

### Cross-camera ID Association

We formulate the cross-camera ID association task as a problem of finding connected components in a graph. We construct the graph based on two observations: 1) The more similar two IDs are, the more likely they are to be the same person. 2) Under the intra-camera supervised setting, each ID has no positive matches within the same camera and at most one positive match in one of the other cameras. According to these observations, we construct an undirected graph  $\mathcal{G} = (\mathcal{V}, \mathcal{E})$  for association, where the vertex set  $\mathcal{V}$  denotes the IDs accumulated over all cameras and the edge set  $\mathcal{E} = \{e(i, j)\}$  indicates whether the  $i$ -th ID and the  $j$ -th ID is a positive pair or not. The edge  $e(i, j)$  is defined by

$$e(i, j) = \begin{cases} 1, & \text{dist}(i, j) < T \wedge \text{cam}(i) \neq \text{cam}(j) \\ & \wedge i \in \mathcal{N}_1(j, \text{cam}(i)) \wedge j \in \mathcal{N}_1(i, \text{cam}(j)); \\ 0, & \text{otherwise.} \end{cases} \quad (6)$$

Here,  $\text{dist}(i, j) = \|\mathcal{K}[i] - \mathcal{K}[j]\|$  calculates the Euclidean distance between two ID centroids stored in the memory bank, and  $i, j \in \{1, \dots, N\}$ .  $T$  is a threshold taken by ascendingly sorting the distances of ID pairs and choosing the  $S$ -th distance value, implying to choose Top  $S$  similar pairs.  $\text{cam}(i)$  represents the camera that the  $i$ -th ID belongs to.  $\mathcal{N}_1(i, \text{cam}(j))$  is the 1-nearest neighbor for ID  $i$  in the camera  $\text{cam}(j)$ .

Once the graph is constructed, we adopt DBSCAN [Ester *et al.*, 1996] to find all connected components. Then all IDs within each component are associated and assigned with a same pseudo identity label. The pseudo labels are further used to update our Re-ID model.

### Re-ID Model Updating

Taking all images and their pseudo labels, we treat the model updating as a fully supervised person Re-ID problem. Therefore, we adopt the simple yet effective architecture in BoT [Luo *et al.*, 2019] to learn the model and meanwhile initialize the feature extraction backbone with the parameters learned in the intra-camera learning stage. The model is trained with the extensively used cross-entropy loss with the label smoothing scheme, termed as an inter-camera ID loss  $\mathcal{L}_{Inter\_ID}$  in our work, together with a batch-hard triplet loss  $\mathcal{L}_{Inter\_Triplet}$  applied to the features output from the GAP layer. Therefore, the total loss for inter-camera learning is:

$$\mathcal{L}_{Inter} = \mathcal{L}_{Inter\_ID} + \mathcal{L}_{Inter\_Triplet}. \quad (7)$$

## 4 Experiments

### 4.1 Experiment Setting

#### Datasets and Evaluation Metrics

We evaluate the proposed method on three large-scale datasets: Market-1501 [Zheng *et al.*, 2015], DukeMTMC-

reID [Ristani *et al.*, 2016; Zheng *et al.*, 2017], and MSMT17 [Wei *et al.*, 2018]. To simulate the ICS setting, we generate intra-camera identity labels based on the provided full annotations. Table 1 lists the numbers of cameras, IDs, and images contained in each dataset, as well as the accumulated total identity number under intra-camera supervision ( $\#ID_{ICS}$ ), the averaged image-per-person (IP) value, together with the averaged image-per-camera-per-person (ICP) value. For performance evaluation, we adopt the Cumulative Matching Characteristic (CMC) and mean Average Precision (mAP), as the common practice.

Dataset	$\#Cam$	$\#ID$	$\#Img$	$\#ID_{ICS}$	IP	ICP
Market-1501	6	751	12,936	3,262	17.23	3.97
DukeMTMC-reID	8	702	16,522	2,196	23.54	7.52
MSMT17	15	1,041	32,621	4,821	31.34	6.77

Table 1: Statistics of each dataset.  $\#Cam$ ,  $\#ID$ ,  $\#Img$ , and  $\#ID_{ICS}$  are the number of cameras, IDs, images, and accumulated IDs under ICS, respectively. IP is the averaged image-per-person value and ICP is the averaged image-per-camera-per-person value.

### Implementation details

We adopt ResNet-50 [He *et al.*, 2016] pre-trained on ImageNet [Krizhevsky *et al.*, 2012] as our feature extraction backbone. Following [Luo *et al.*, 2019], we remove the last spatial down-sampling operation in the backbone to increase the size of feature maps, and add a batch normalization (BN) layer after GAP.

During both intra- and inter-camera learning, images are resized to  $256 \times 128$  and performed random flipping, random cropping, and random erasing for data augmentation. The initial learning rate is 0.00035 and divided by 10 after 40 and 70 epochs. We choose Adam [Kingma and Ba, 2014] as the optimizer with weight decay 0.0005. Training batch size is 64, with randomly selected 16 IDs and 4 images for each ID. In intra-camera learning, images within each mini-batch are sampled according to the per-camera labels, and the total number of epochs is 50. The updating rate  $\mu$  in Equation (1) is set to 0.5, and the temperature  $\tau$  in Equation (2) is set to 0.067 (i.e.  $1/15$ ). The margins  $m_1$  and  $m_2$  in Equation (4) are both empirically set to 0.3. In inter-camera learning, images in each mini-batch are sampled according to the generated pseudo ID labels. The total number of epochs is set to 120. In graph construction, we select Top  $S$  similar pairs as candidates for edge linking, in which  $S$  is empirically set to be the same number as  $\#ID_{ICS}$  listed in Table 1. Each experiment runs 5 times and we report the averaged performance to ensure the reliability of the results.

## 4.2 Ablation Study

### Effectiveness of The Camera-specific Non-parametric Classifiers in Intra-camera Learning

We conduct a series of experiments to validate the effectiveness of each component proposed in our method. First, we are curious about how well the camera-specific non-parametric classifiers perform. Therefore, three model variants are investigated, including  $\mathcal{M}_1$ : a multi-branch network structure [Zhu *et al.*, 2019], in which each branch uses a classifier parameterized by a FC layer and optimized with a

cross-entropy ID loss, for intra-camera learning;  $\mathcal{M}_2$ : a non-parametric classifier but not camera-specific, that is, any image can be classified into all accumulated ID classes;  $\mathcal{M}_3$ : the proposed camera-specific non-parametric classifiers with the intra-camera ID loss only.

Models	Market1501		DukeMTMC-ReID		MSMT17	
	mAP	Rank-1	mAP	Rank-1	mAP	Rank-1
$\mathcal{M}_1$	55.0	76.8	58.9	75.3	25.1	50.7
$\mathcal{M}_2$	30.7	45.5	29.1	33.3	6.0	10.4
$\mathcal{M}_3$	<b>69.2</b>	<b>86.1</b>	<b>61.9</b>	<b>78.0</b>	<b>25.7</b>	<b>52.1</b>
$\mathcal{M}_4$	71.9	86.8	64.0	79.1	28.1	54.3
$\mathcal{M}_5$	<b>72.3</b>	<b>87.5</b>	<b>64.7</b>	<b>79.7</b>	<b>28.9</b>	<b>55.5</b>
$\mathcal{M}_6$	<b>83.6</b>	<b>93.1</b>	<b>72.0</b>	<b>83.6</b>	<b>31.3</b>	<b>57.7</b>
$\mathcal{M}_7$	85.9	94.1	77.2	87.4	52.2	75.3

Table 2: Comparison of the different model variants.  $\mathcal{M}_1$ - $\mathcal{M}_5$  are all intra-camera learning models, in which  $\mathcal{M}_1$  is a multi-branch parametric classification architecture,  $\mathcal{M}_2$  is a camera-agnostic non-parametric classifier, and  $\mathcal{M}_3$  is our proposed camera-specific non-parametric classifiers.  $\mathcal{M}_4$  is  $\mathcal{M}_3$  with an additional triplet loss and  $\mathcal{M}_5$  is  $\mathcal{M}_3$  with the proposed quintuplet loss.  $\mathcal{M}_6$  is the full model containing both intra- and inter-camera learning.  $\mathcal{M}_7$  is a fully supervised version.

Table 2 presents the comparison results in terms of mAP(%) and Rank-1(%). From the results we observe that the camera-specific non-parametric classifiers ( $\mathcal{M}_3$ ) outperform the camera-agnostic counterpart ( $\mathcal{M}_2$ ) by a great margin, showing that the camera-specific constraint plays an important role. In addition, the camera-specific non-parametric classifiers ( $\mathcal{M}_3$ ) perform consistently better than the parametric counterpart ( $\mathcal{M}_1$ ) on all datasets. Especially, it improves the performance by a significant margin (mAP +14.2% and Rank-1 +9.3%) on Market1501 which has a smaller ICP value than the other two datasets, as reported in Table 1. It indicates that the non-parametric classifier is superior when identity classes contain fewer examples.

### Effectiveness of The Quintuplet Loss in Intra-camera Learning

When validating the effectiveness of the proposed quintuplet loss, we investigate two model variants, which are  $\mathcal{M}_4$ : the camera-specific non-parametric classifiers with the intra-camera ID loss and a batch-hard triplet loss [Hermans *et al.*, 2017]; and  $\mathcal{M}_5$ : the camera-specific non-parametric classifiers with the intra-camera ID loss and the proposed quintuplet loss. From the results reported in Table 2, we observe that both models  $\mathcal{M}_4$  and  $\mathcal{M}_5$  gain considerable improvements when compared to  $\mathcal{M}_3$  that does not use any metric learning loss. Moreover, the model using the quintuplet loss ( $\mathcal{M}_5$ ) performs consistently better than the one using the triplet loss ( $\mathcal{M}_4$ ), demonstrating that it is effective to leverage information from both mini-batch and the global batch.

### Effectiveness of The Inter-camera Learning Part

After the comparisons of all intra-camera learning components, we validate the effectiveness of the inter-camera learning part. To this end, we add this part on  $\mathcal{M}_5$  to get the full model  $\mathcal{M}_6$  and present the results in Table 2. Meanwhile, Table 2 also provides the results obtained by training the inter-

Methods	Market1501				DukeMTMC-ReID				MSMT17			
	mAP	R1	R5	R10	mAP	R1	R5	R10	mAP	R1	R5	R10
<b>Fully supervised</b>												
OSNet [Zhou <i>et al.</i> , 2019]	84.9	94.8	-	-	73.5	88.6	-	-	52.9	78.7	-	-
DGNet [Zheng <i>et al.</i> , 2019]	86.0	94.8	-	-	74.8	86.6	-	-	52.3	77.2	87.4	90.5
BoT [Luo <i>et al.</i> , 2019]	85.9	94.5	-	-	76.4	86.4	-	-	-	-	-	-
PCB [Sun <i>et al.</i> , 2018]	81.6	93.8	-	-	69.2	83.3	-	-	40.4	68.2	-	-
<b>Unsupervised</b>												
ECN [Zhong <i>et al.</i> , 2019a]	43.0	75.1	87.6	91.6	40.4	63.3	75.8	80.4	10.2	30.2	41.5	46.8
AE [Ding <i>et al.</i> , 2019]	58.0	81.6	91.9	94.6	46.7	67.9	79.2	83.6	11.7	32.3	44.4	50.1
BUC [Lin <i>et al.</i> , 2019]	38.3	66.2	79.6	84.5	27.5	47.4	62.6	68.4	-	-	-	-
UGA [Wu <i>et al.</i> , 2019]	70.3	87.2	-	-	53.3	75.0	-	-	21.7	49.5	-	-
<b>Intra-camera supervised</b>												
MTML [Zhu <i>et al.</i> , 2019]	65.2	85.3	-	96.2	50.7	71.7	-	86.9	18.6	44.1	-	63.9
PCSL [Qi <i>et al.</i> , 2019b]	69.4	87.0	94.8	96.6	53.5	71.7	84.7	88.2	20.7	48.3	62.8	68.6
ACAN [Qi <i>et al.</i> , 2019a]	50.6	73.3	87.6	91.8	45.1	67.6	81.2	85.2	12.6	33.0	48.0	54.7
Precise-ICS: $\mathcal{M}_5$ (Ours)	72.3	87.5	95.1	97.2	64.7	79.7	89.2	92.4	28.9	55.5	69.3	75.0
Precise-ICS: $\mathcal{M}_6$ (Ours)	83.6	93.1	97.8	98.6	72.0	83.6	92.6	94.7	31.3	57.7	71.1	76.3

Table 3: Comparison with state-of-the-art methods. ‘Precise-ICS’ is the approach proposed in this work,  $\mathcal{M}_5$  refers to the model with our intra-camera learning only and  $\mathcal{M}_6$  is our full model considering both intra- and inter-camera learning. Note that no re-ranking is used during training or evaluation.

Model	Market1501		DukeMTMC-ReID		MSMT17	
	Prec	Rec	Prec	Rec	Prec	Rec
$\mathcal{M}_6$	96.4	75.9	90.1	74.3	86.3	38.3

Table 4: Precision and recall of the ID pairs associated by our approach.

camera learning branch in our network with entire ground-truth labels, which in essence is the fully supervised counterpart model  $\mathcal{M}_7$ . This model indicates the upper bound performance that can be achieved by our Re-ID network architecture.

The results show that our inter-camera learning part makes significant improvements, especially on Market1501 and DukeMTMC-ReID. The improvements are benefited from our intra-camera learning components that equip the Re-ID model with an outstanding discrimination capability, enabling us to gain reliable ID association results. As shown in Table 4, the precision and recall of the ID pairs associated by our approach are pretty high on Market1501 and DukeMTMC-ReID, but relatively low on MSMT17 that is a dataset much more complicated than the others. The correctly associated IDs make the inter-camera learning effective. As indicated in Table 2, the performance of our full model ( $\mathcal{M}_6$ ) is even close to the supervised model ( $\mathcal{M}_7$ ) on Market1501 and DukeMTMC-ReID.

### 4.3 Comparison with the State-of-the-Arts

In this section, we compare our approach (named as Precise-ICS) with all existing ICS person Re-ID methods, including MTML [Zhu *et al.*, 2019], PCSL [Qi *et al.*, 2019b] and ACAN [Qi *et al.*, 2019a]. The comparison results are presented in Table 3 in terms of mAP(%), Rank-1(%), Rank-5(%), and Rank-10(%). From the results we observe that the proposed approach outperforms the other ICS methods by a great margin. More specifically, the mAP is 14.2%, 18.5%,

and 10.6% higher and the Rank-1 accuracy is 6.1%, 11.9%, and 9.4% higher than the best performances obtained by other methods on Market1501, DukeMTMC-ReID, and MSMT17 respectively. Even the model using only the intra-camera learning part (Precise-ICS:  $\mathcal{M}_5$ ) performs consistently better than all existing ICS methods, indicating that the proposed components in our intra-camera learning can exploit per-camera labels much more thoroughly.

In addition, we also compare our work with state-of-the-art methods under different supervision settings, including four fully supervised methods (OSNet [Zhou *et al.*, 2019], DGNet [Zheng *et al.*, 2019], BoT [Luo *et al.*, 2019], PCB [Sun *et al.*, 2018]) and four unsupervised methods (ECN [Zhong *et al.*, 2019a], AE [Ding *et al.*, 2019], BUC [Lin *et al.*, 2019], UGA [Wu *et al.*, 2019]). As expected, our approach achieves much higher performance than the unsupervised methods no matter if they transfer knowledge from extra datasets or not. Meanwhile, our approach is better than PCB [Sun *et al.*, 2018], which is an effective fully supervised method developed two years ago. Our approach is even comparable to recent supervised methods on Market1501 and DukeMTMC-ReID. The results demonstrate the potential for the ICS Re-ID task to achieve high Re-ID performance while dramatically reduce labeling cost, making this supervision setting more scalable to real-world applications.

## 5 Conclusion

In this paper, we have proposed a new approach to address the person Re-ID problem under intra-camera supervision. The proposed network consists of a simple yet effective feature extraction backbone, together with two branches for intra- and inter-camera learning respectively. According to the per-camera labeling nature of ICS, we propose camera-specific non-parametric classifiers and a hybrid mining quintuplet loss

for intra-camera learning. The designed components exploit per-camera labels thoroughly so that our intra-camera learning part only can perform better than existing ICS methods. Benefited from the discrimination ability gained in this part, the inter-camera learning module boosts the Re-ID performance further by mining ID relationship across cameras. Our full model outperforms all ICS methods by a large margin, greatly reducing the gap to the fully supervised counterparts.

## References

- [Chen *et al.*, 2018] Yanbei Chen, Xiatian Zhu, and Shaogang Gong. Semi-supervised deep learning with memory. In *ECCV*, 2018.
- [Chen *et al.*, 2019] Tianlong Chen, Shaojin Ding, Jingyi Xie, Ye Yuan, Wuyang Chen, Yang Yang, Zhou Ren, and Zhangyang Wang. Abd-net: Attentive but diverse person re-identification. In *ICCV*, 2019.
- [Deng *et al.*, 2018] Weijian Deng, Liang Zheng, Qixiang Ye, Yi Yang, and Jianbin Jiao. Image-image domain adaptation with preserved self-similarity and domain-dissimilarity for person re-identification. In *CVPR*, 2018.
- [Ding *et al.*, 2019] Yuhang Ding, Hehe Fan, Mingliang Xu, and Yi Yang. Adaptive exploration for unsupervised person re-identification. *arXiv preprint arXiv:1907.04194*, 2019.
- [Ester *et al.*, 1996] Martin Ester, Hans-Peter Kriegel, Jiirg Sander, and Xiaowei Xu. A density-based algorithm for discovering clusters in large spatial databases with noise. In *KDD*, 1996.
- [Fan *et al.*, 2018] Hehe Fan, Liang Zheng, Chenggang Yan, and Yi Yang. Unsupervised person re-identification: Clustering and fine-tuning. *ACM Transactions on Multimedia Computing, Communications, and Applications*, 14(4):83, 2018.
- [He *et al.*, 2016] Kaiming He, Xiangyu Zhang, Shaoqing Ren, and Jian Sun. Deep residual learning for image recognition. In *CVPR*, 2016.
- [Hermans *et al.*, 2017] Alexander Hermans, Lucas Beyer, and Bastian Leibe. In defense of the triplet loss for person re-identification. *arXiv preprint arXiv:1703.07737*, 2017.
- [Kingma and Ba, 2014] Diederik P. Kingma and Jimmy Lei Ba. Adam: A method for stochastic optimization. *arXiv preprint arXiv:2014*, 2014.
- [Krizhevsky *et al.*, 2012] Alex Krizhevsky, Ilya Sutskever, and Geoffrey E Hinton. Imagenet classification with deep convolutional neural networks. In *Advances in neural information processing systems*, pages 1097–1105, 2012.
- [Lin *et al.*, 2019] Yutian Lin, Xuanyi Dong, Liang Zheng, Yan Yan, and Yi Yang. A bottom-up clustering approach to unsupervised person re-identification. In *AAAI*, 2019.
- [Luo *et al.*, 2019] Hao Luo, Youzhi Gu, Xingyu Liao, Shenqi Lai, and Wei Jiang. Bag of tricks and a strong baseline for deep person re-identification. In *CVPRW*, 2019.
- [Qi *et al.*, 2019a] Lei Qi, Lei Wang, Jing Huo, Yinghuan Shi, and Yang Gao. Adversarial camera alignment network for unsupervised cross-camera person re-identification. *arXiv preprint arXiv:1908.00862*, 2019.
- [Qi *et al.*, 2019b] Lei Qi, Lei Wang, Jing Huo, Yinghuan Shi, and Yang Gao. Progressive cross-camera soft-label learning for semi-supervised person re-identification. *arXiv preprint arXiv:1908.05669*, 2019.
- [Ristani *et al.*, 2016] Ergys Ristani, Francesco Solera, Roger Zou, Rita Cucchiara, and Carlo Tomasi. Performance measures and a data set for multi-target, multi-camera tracking. In *ECCV*, 2016.
- [Sun *et al.*, 2018] Yifan Sun, Liang Zheng, Yi Yang, Qi Tian, and Shengjin Wang. Beyond part models: Person retrieval with refined part pooling (and a strong convolutional baseline). In *ECCV*, pages 480–496, 2018.
- [Wei *et al.*, 2018] Longhui Wei, Shiliang Zhang, Wen Gao, and Qi Tian. Person transfer gan to bridge domain gap for person re-identification. In *CVPR*, 2018.
- [Wu *et al.*, 2018] Zhirong Wu, Yuanjun Xiong, Stella X. Yu, and Dahua Lin. Unsupervised feature learning via non-parametric instance discrimination. In *CVPR*, 2018.
- [Wu *et al.*, 2019] Jinlin Wu, Yang Yang, Hao Liu, Shengcai Liao, Zhen Lei, and Stan Z. Li. Unsupervised graph association for person re-identification. In *ICCV*, 2019.
- [Xiao *et al.*, 2017] Tong Xiao, Shuang Li, Bochao Wang, Liang Lin, and Xiaogang Wang. Joint detection and identification feature learning for person search. In *CVPR*, 2017.
- [Yang *et al.*, 2019] Qize Yang, Ancong Wu, and Wei-Shi Zheng. Deep semi-supervised person re-identification with external memory. In *ICME*, 2019.
- [Zhai *et al.*, 2019] Yao Zhai, Xun Guo, Yan Lu, and Houqiang Li. In defense of the classification loss for person re-identification. In *CVPRW*, 2019.
- [Zhang *et al.*, 2019] Zhizheng Zhang, Cuiling Lan, Wenjun Zeng, and Zhibo Chen. Densely semantically aligned person re-identification. In *CVPR*, 2019.
- [Zheng *et al.*, 2015] L. Zheng, L. Shen, L. Tian, S. Wang, J. Wang, and Q. Tian. Scalable person re-identification: A benchmark. In *ICCV*, 2015.
- [Zheng *et al.*, 2017] Zhedong Zheng, Liang Zheng, and Yi Yang. Unlabeled samples generated by gan improve the person re-identification baseline in vitro. In *ICCV*, 2017.
- [Zheng *et al.*, 2019] Zhedong Zheng, Xiaodong Yang, Zhiding Yu, Liang Zheng, Yi Yang, and Jan Kautz. Joint discriminative and generative learning for person re-identification. In *CVPR*, 2019.
- [Zhong *et al.*, 2019a] Zhun Zhong, Liang Zheng, Zhiming Luo, Shaozi Li, and Yi Yang. Invariance matters: Exemplar memory for domain adaptive person re-identification. In *CVPR*, 2019.
- [Zhong *et al.*, 2019b] Zhun Zhong, Liang Zheng, Zhiming Luo, Shaozi Li, and Yi Yang. Learning to adapt invariance

in memory for person re-identification. *arXiv preprint arXiv:1908.00485*, 2019.

[Zhou *et al.*, 2019] Kaiyang Zhou, Yongxin Yang, Andrea Cavallaro, and Tao Xiang. Omni-scale feature learning for person re-identification. In *ICCV*, 2019.

[Zhu *et al.*, 2019] Xiangping Zhu, Xiatian Zhu, Minxian Li, Vittorio Murino, and Shaogang Gong. Intra-camera supervised person re-identification: A new benchmark. In *ICCVW*, 2019.